ELSEVIER

Journal of Photochemistry and Photobiology A: Chemistry 153 (2002) 1–10

Journal of Photochemistry and Photobiology A:Chemistry

www.elsevier.com/locate/jphotochem

Photochemistry of concentrated sulfuric acid in the presence of SO_2 and Fe(II), and implications for the cloud chemistry of Venus

G.A. Rowland [a], R. van Eldik [b], L.F. Phillips [a,*]

[a] *Chemistry Department, University of Canterbury, Christchurch, New Zealand*
[b] *Institute for Inorganic Chemistry, University of Erlangen-Nürnberg, 91058 Erlangen, Germany*

Received 1 July 2002; received in revised form 29 July 2002; accepted 5 August 2002

Abstract

Measurements of the conversion of trace amounts of Fe(II) to Fe(III) have been used to monitor the progress of photochemistry in bulk samples of concentrated sulfuric acid under 248 nm laser irradiation. Because sulfuric acid does not undergo single-photon absorption at 248 nm, and because conditions that could promote multiphoton absorption were absent, primary processes in this system must involve the additives or other impurities. Major primary processes in our system are considered to be production of H atoms by photolysis of complex ions containing Fe(II), of SO_3^- radical ions and atomic hydrogen by photolysis of HSO_3^-, and of SO_4^- radical ions by photolysis of complex ions containing Fe(III). Kinetic modeling shows that processes involving Fe(III) are normally less important in our system than processes involving Fe(II). Independently of which primary process is dominant, secondary reactions occur which are similar to those that result in the formation of acid rain in Earth's troposphere. These secondary processes lead to removal of oxygen in a very fast reaction with SO_3^- and thence to production of HSO_5^-, the stable anion of peroxymonosulfuric acid, which can oxidize CO to CO_2. Our results imply that photochemical reactions in the sulfuric acid clouds of Venus can affect the composition of the atmosphere at high altitudes, by removing O_2 and CO and regenerating CO_2, and so help stabilize the 96% CO_2 atmosphere of Venus against photolysis by solar ultraviolet radiation.

Keywords: Photochemistry; Concentrated sulfuric acid; Venus

1. Introduction

The current state of knowledge of the chemistry of the Venus atmosphere is little changed from the account given in the book by Krasnopolsky [1]. The atmosphere is composed mainly of carbon dioxide (ca. 95%) and nitrogen (4%), and there is a dense cloud cover, comprised mostly of droplets of concentrated sulfuric acid, arranged in several more-or-less distinct layers over the altitude range from about 48–62 km. Vertical exchange of material is thought to be facilitated by a continuous rain of concentrated acid droplets from the upper layers, the droplets evaporating near the bottom of the clouds, with a compensating upward flow of gas. The gas composition in the upper cloud layer is notable for the presence of very little O_2 (spectroscopic upper limit ∼1 ppm), together with small amounts of CO (∼50 ppm) and SO_2 (∼50 ppm). Hydrogen halides, to the extent of a few parts per million, are also present above the clouds, as was first demonstrated by earth-based spectroscopy [2], and Prinn [3] has proposed a gas-phase mechanism involving reactions of chlorine-containing species to account for the evident stability of the CO_2 atmosphere in the presence of intense photolysing radiation from the sun. This mechanism and others have been incorporated in numerical models of the Venus mesosphere, of which the most successful appear to be those of Yung and DeMore [4]. The same question arises in connection with the CO_2 atmosphere of Mars, but on Mars there is sufficient water available for CO_2 to be regenerated by the reaction of OH with CO, a process which is not significant on Venus.

In his book, Krasnopolsky adopts the very low spectroscopic upper limit for the concentration of O_2 on Venus, in preference to the ∼20 ppm values found by gas chromatographs aboard the Pioneer and Venera probes, and comments that none of the models succeeds in reproducing this low concentration. Krasnopolsky also discusses the evidence for the presence of iron salts such as $FeCl_3$ and $Fe_2(SO_4)_3$ in the lower cloud layers. His estimate of the upward flux of $FeCl_3$ is about 1% of the upward flux of H_2SO_4. If Krasnopolsky's arguments, which unfortunately are based on fairly limited experimental evidence, are correct, they

* Corresponding author.
E-mail address: phillips@chem.canterbury.ac.nz (L.F. Phillips).

1010-6030/02/$ – see front matter © 2002 Elsevier Science B.V. All rights reserved.
PII: S1010-6030(02)00303-9

imply that iron salts are also present in the clouds at high altitudes.

Our work addresses the question of whether cloud photochemistry might play a part in maintaining the composition of the Venus atmosphere [5–8]. Initial qualitative experiments, which showed that CO could be oxidized to CO_2 by 193 nm radiation in the presence of a sulfuric acid aerosol [5], were followed by quantum yield measurements for CO_2 and SO_2 [6]. These measurements showed that, whereas the yield of CO_2 was always positive, the yield of SO_2 could be either positive or negative. During the quantum yield measurements, small flows of CO_2 and SO_2 were introduced downstream of the photochemical reactor to serve as mass-spectrometric standards, and a negative yield corresponded to removal of some of the added SO_2 by reaction with a long-lived species contained in the aerosol. This long-lived species was tentatively identified as peroxymonosulfuric acid, H_2SO_5 (Caro's acid), but there remained considerable uncertainty about the details of the process by which it was formed. It is important to note that, in these experiments, the aerosol was generated by mixing two gas streams that contained H_2O and SO_3, in the absence of SO_2, so that neither sulfite ions nor metal salts could have been involved in the primary process.

Subsequent experimental and theoretical work [7] led to the conclusion that sulfuric acid does not undergo single-photon absorption at 193 nm, and that the observed aerosol photochemistry must therefore have been the result of multiphoton absorption, due to quasi-focusing of the laser radiation by morphology-dependent resonance modes of the droplets, similar to those discussed by Chang et al. [9]. Hence, we undertook a variety of experiments using bulk acid solutions to avoid multiphoton effects, work which led eventually to the study of photochemical interconversion of Fe(II) and Fe(III) which is the subject of the present paper. A preliminary account of this work has appeared elsewhere [8]. As noted in [8], we have made no attempt to incorporate cloud photochemistry into numerical models of the atmosphere of Venus and we have no plans to do so.

Photochemical reactions of sulfur dioxide and related species in *aqueous* aerosol droplets have been studied in considerable detail as part of the HALIPP program [10] which deals with *heterogeneous and liquid-phase processes* (hence the acronym) and is part of the EUROTRAC program on the transport and chemical transformations of pollutants in the troposphere, with particular emphasis on acid rain. A major aim of this work was to elucidate the mechanism of oxidation of aqueous SO_2 to sulfuric acid in the presence of catalytic amounts of transition metals, especially manganese and iron, dissolved in the aerosols. As a result, for many of the processes of interest in connection with the clouds of Venus, rate constants and quantum yields have been measured or compiled as part of the HALIPP project. We have constructed a mechanism for the present experimental system on the basis of the HALIPP work and have carried out numerical integrations of the resulting rate equations. Results obtained for dilute aqueous systems at room temperature are not directly transferable to concentrated sulfuric acid solutions, especially if the sulfuric acid is at 250 K, the temperature near the top of the Venus clouds, but they can provide a useful guide to likely primary processes and an indication of which secondary reactions can be expected to be fast. For diffusion-limited reactions the rate constant varies inversely with viscosity, so such reactions will be slower by a factor of 275 in 100% sulfuric acid at 250 K than in water at 300 K (using viscosity data extrapolated from Liler [11]), and slower by a factor of about 25 at 300 K. Other factors, such as differences in the dielectric constant and in acid dissociation constants, will also play a part. Our numerical calculations used rate constants for aqueous solutions at room temperature as listed in [10], with no correction for viscosity, and therefore can have only qualitative significance. Nevertheless, they provide a reasonably secure basis for our belief that cloud photochemistry plays a significant part in conferring a remarkable degree of photochemical stability on the CO_2 atmosphere of Venus.

2. Experimental

The Fe(II)/Fe(III) experiments used bulk samples of concentrated sulfuric acid (usually 98 wt.% acid), and the samples were irradiated with a 248 nm KrF laser (Lumonics model EX-744). The laser was normally operated at a repetition frequency of 20 Hz, with pulse energies around 100 mJ, as measured with a Coherent 100E power meter, distributed over an approximately 2 cm^2 cross-section of the photolysis cell. Before each photolysis run, the acid was largely freed of dissolved oxygen by bubbling research grade argon through it for several hours. Crystals of the iron salt or other additive were then introduced, and the solution was mixed by further bubbling and shaking. The resulting solution was transferred to a 2 cm^2 Suprasil cell in which the depth of liquid was adjusted so that almost all of the acid sample was in the laser irradiation zone. In most of the experiments, ferrous ammonium sulfate, sufficient to give a final Fe(II) concentration near 10^{-4} mol L^{-1}, was added to the acid, the concentration of iron salt being chosen so as to give an easily measurable change in absorption over the 2 cm path-length at right angles to the laser beam. In some experiments S(IV) was introduced in the form of sodium sulfite and, in a few experiments, CO was added as calcium formate. The interconversion of Fe(II) and Fe(III) was monitored at right angles to the laser beam with a deuterium lamp, a monochromator set at 248 nm, and a photomultiplier. The photomultiplier signal corresponding to the intensity of transmitted light at 248 nm was taken to a computer by way of a Keithley picoammeter and an ac/dc converter. The results of irradiation were generally reproducible for irradiation times up to about 20 min, after which they tended to diverge, as shown in Fig. 1, an effect which was associated with the appearance of visible

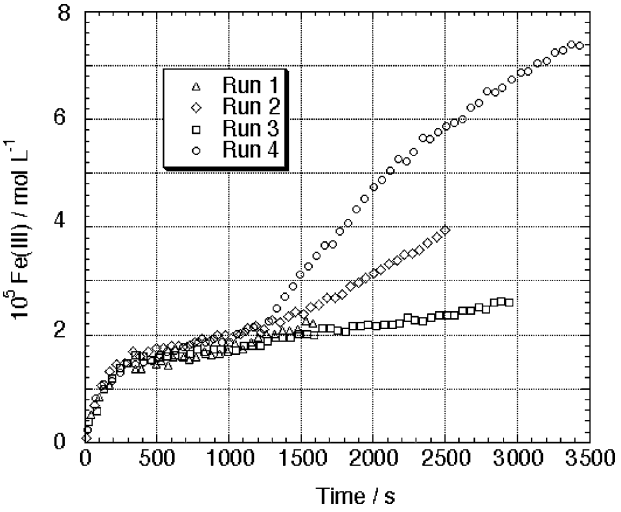

Fig. 1. Photolysis of 2.22×10^{-4} M Fe(II) in 98 wt.% sulfuric acid, laser power = 0.6 W.

striations due to uneven heating of the solution. For this reason, most experiments were terminated after 10 min. Ferric salts do not dissolve readily in concentrated sulfuric acid, so Fe(III) solutions were prepared by oxidizing Fe(II) with crystalline sodium peroxymonosulfate (PMS). At the end of each photolysis run with Fe(II), the iron in the sample was entirely converted to Fe(III) by addition of PMS and its concentration was measured with a spectrophotometer. For a number of runs, the concentration of dissolved oxygen was measured before and after irradiation with a Lazar Research Laboratories dissolved-oxygen electrode. Unfortunately it was not practicable to measure the dissolved-oxygen concentration in real time, during irradiation. When oxygen was introduced, this was done by bubbling the gas for an hour or more after the initial degassing with argon. In experiments where S(IV) was introduced as sodium sulfite, it would largely have been present in the form of bisulfite ion HSO_3^- and solvated SO_2 in the initial solution. Unfortunately, the acid dissociation constants of sulfurous acid in this medium are unknown. When Fe(II) was introduced it was partly converted to S(IV) and Fe(III) by a reaction of the type

$$2Fe^{2+} + H_2SO_4 + 2H^+ \rightarrow 2Fe^{3+} + SO_2 + 2H_2O \qquad (1)$$

for which the standard reduction potentials correspond to a value of 6.54×10^{-23} for the equilibrium constant in water at 25 °C. Although the equilibrium constant is very small in water, the low activities of water and SO_2 in concentrated sulfuric acid evidently allow reaction (1) to proceed to a significant extent. The reaction does not reach equilibrium immediately, measurable changes in the Fe(III) absorption being observed over a period of several hours. For a sample in which the only SO_2 present is that produced by reaction (1), so that the SO_2 activity can be estimated from the activity of Fe^{3+}, spectroscopic measurements of the ratio of Fe(III) to Fe(II), combined with existing data for the activity of H_2O, suggest themselves as an alternative method of measuring the activity of hydrogen ions in highly concentrated H_2SO_4. The distribution of S(IV), Fe(II) and Fe(III) among the various possible complexed, protonated and solvated species in these solutions is unknown, but this does not affect the present discussion provided the various complexes are readily interconverted, as is expected to be the case.

Absorption spectra were measured with a 1 cm cell in a GBC UV-Vis 920 spectrophotometer. Spectra of Fe(III) and S(IV) in 98 wt.% H_2SO_4 are shown in Fig. 2. Both absorbers gave good Beer's Law plots for absorption at 248 nm. The Fe(III) spectrum is a broad, double hump; the S(IV) spectrum consists of a broad absorption with a small absorption peak at 280 nm and a stronger peak at 198 nm. We consider this to be a real absorption peak, rather than an artefact of the spectrometer, because this feature is not present in the Fe(III) spectrum and because gaseous SO_2 has a peak in the same region. The spectrum of Fe(II) could not be observed under these conditions because the absorption was dominated by the Fe(III) from reaction 1, and we can report only an upper limit of $\sim$4 L (mol cm)$^{-1}$ for the molar absorption coefficient of Fe(II) at 248 nm in 98% acid. There is no reason to suppose that something drastic could have happened to the transition moment, so we conclude that the Fe(II) absorption is relatively broad and featureless in concentrated sulfuric acid.

3. Results

Photochemical production of H_2SO_5 (and of H_2O_2, which is always present in H_2SO_5) was demonstrated by using a microwave-powered atomic iodine lamp, similar to that described by Brewer and Tellinghuisen [12], to irradiate 2.5 ml samples of AnalaR analytical reagent grade sulfuric acid, containing small amounts of S(IV) as a photosensitizer, for periods of up to 4 h. The lamp gave atomic iodine emission at a number of wavelengths from 206.2 nm down, the most intense line being at 178.3 nm. The cell containing the acid sample was immersed in an ice bath during irradiation, and a steady flow of argon was maintained over the liquid surface, in an effort to carry away gaseous products such as SO_2 which could limit the production of H_2SO_5. The results suggest that this effort was not very successful. The irradiated solutions were diluted to an acid strength of 5 mol L^{-1} before being analyzed for H_2O_2 and H_2SO_5 by reaction with Fe(II) and Ce(IV), as in the method of Mariano [13] but omitting Mariano's procedure for determining $H_2S_2O_8$. The typical results shown in Fig. 3 indicate that H_2O_2 and H_2SO_5 were produced in this system, but that the concentrations of both H_2O_2 and H_2SO_5 rapidly reached a maximum value, after which further irradiation was either ineffective (as for H_2SO_5) or counter-productive (as for H_2O_2). The possibility exists that some or all of the missing H_2O_2 and H_2SO_5 had been converted to $H_2S_2O_8$, whose concentration was not measured.

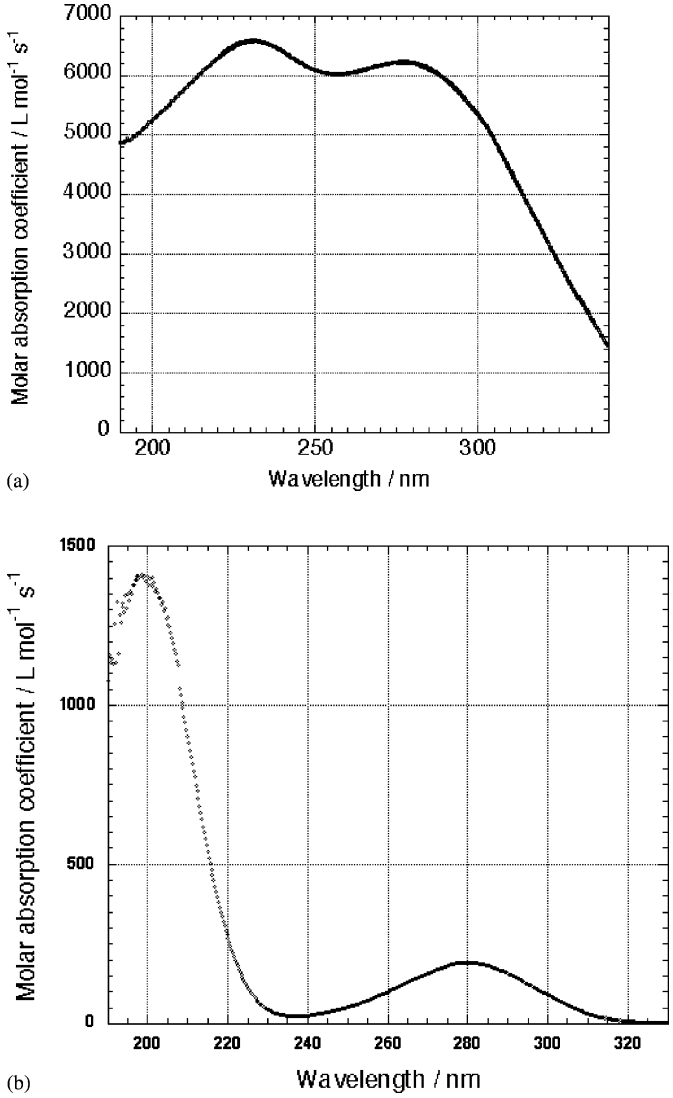

Fig. 2. (a) Absorption spectrum of Fe(III) in 98 wt.% sulfuric acid. (b) Absorption spectrum of S(IV) in 98% sulfuric acid.

Spectroscopic observations of the conversion of Fe(II) to Fe(III) were used to monitor the progress of photochemical reaction in most of the experiments. Fig. 4 shows the growth of Fe(III) absorption during 248 nm irradiation for three initial Fe(II) concentrations. The initial rate of growth is a linear function of the initial concentration of Fe(II) (see Fig. 5) and is approximately proportional to the incident light intensity, which implies that there is a primary process involving Fe(II). The quantum yield for conversion of Fe(II) to Fe(III) is typically 1% at the start of the photolysis.

Bubbling O_2 through the solution prior to photolysis produced a small but definite increase in the initial rate of conversion of Fe(II) to Fe(III). The results of addition of SO_2 (in the form of sulfite) were more equivocal, in that there was an initial positive effect on the conversion rate (Fig. 6), but there was a low threshold above which addition of further sulfite made little or no difference. This is consistent with the existence of a primary process involving sulfite, which is also implied by our experiments with the atomic iodine lamp. Such processes are already known from the HALIPP work.

There is a slight complication in connection with the experiments involving sulfite addition, in that this is the normal method of removing dissolved oxygen from aqueous solutions during calibration of an oxygen-sensitive electrode, so that sulfite addition might have affected the nature of secondary processes in our system. However, our experiments with the dissolved-oxygen electrode indicate that sulfite addition is not very effective in removing dissolved oxygen from concentrated sulfuric acid. Even in dilute acid, it is generally preferable to use dithionite, which reacts very rapidly with dissolved oxygen rather than sulfite, which reacts slowly. The electrode measurements were unequivocal in showing that irradiation produced a significant decrease

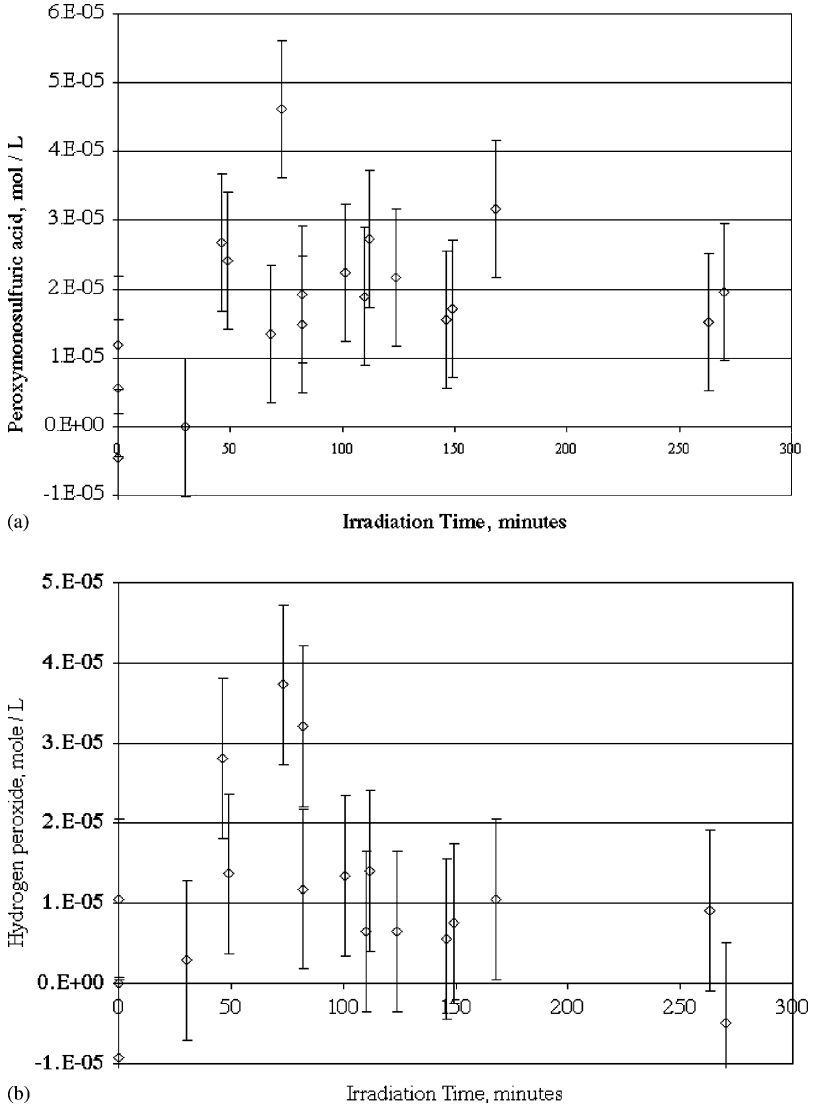

Fig. 3. (a) Concentration of H_2SO_5 as a function of time during 178 nm photolysis of 98% sulfuric acid containing a trace of SO_2 as photosensitizer. (b) Concentration of H_2O_2 as a function of time during 178 nm photolysis of 98% sulfuric acid containing a trace of SO_2 as photosensitizer.

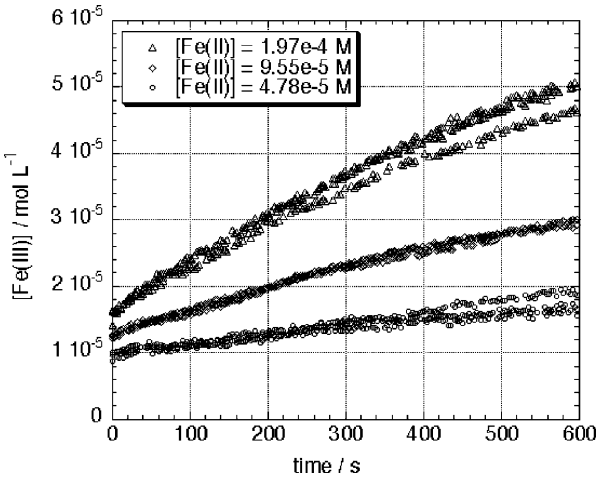

Fig. 4. Growth of [Fe(III)] during photolysis for three different initial Fe(II) concentrations.

in the concentration of O_2, but it is not possible to express this result as a quantum yield because the readings given by the electrode, which was never intended for use in concentrated sulfuric acid, were time-dependent with a very long time constant, and hence were very subject to errors arising from slow drifts.

Addition of small amounts of CO as sodium formate had no detectable effect on the rate of conversion of Fe(II) to Fe(III).

When Fe(III) was photolysed with no Fe(II) initially present, the 248 nm absorption decreased upon irradiation, as shown in Fig. 7, which indicates that there is also a primary process involving the Fe(III) from reaction 1. For mixtures of Fe(II) and Fe(III), the changeover from producing Fe(III) to photolysing Fe(III) occurs when [Fe(III)] is between 0.3 and 0.35 of the total Fe salt present. At concentration ratios in the changeover region, 248 nm photolysis has little or no effect on the extent of light absorption by Fe(III).

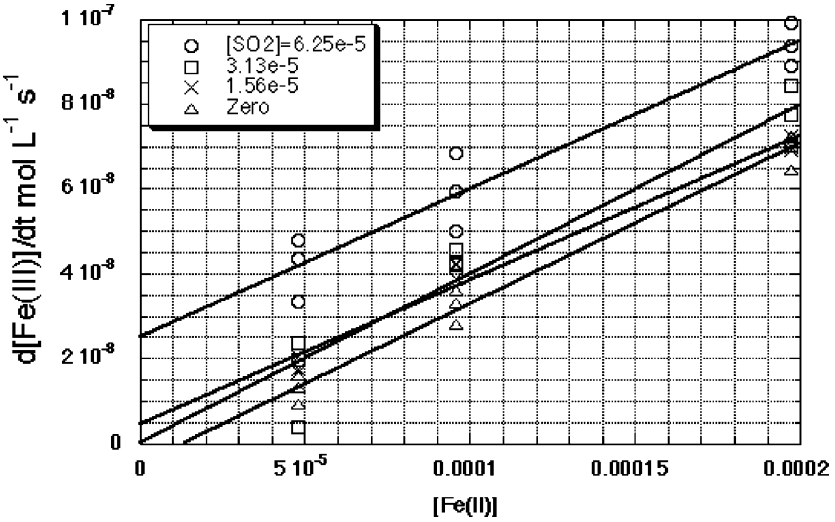

Fig. 5. Initial slope of [Fe(III)] vs. time plot, vs. initial [Fe(II)] at constant [S(IV)].

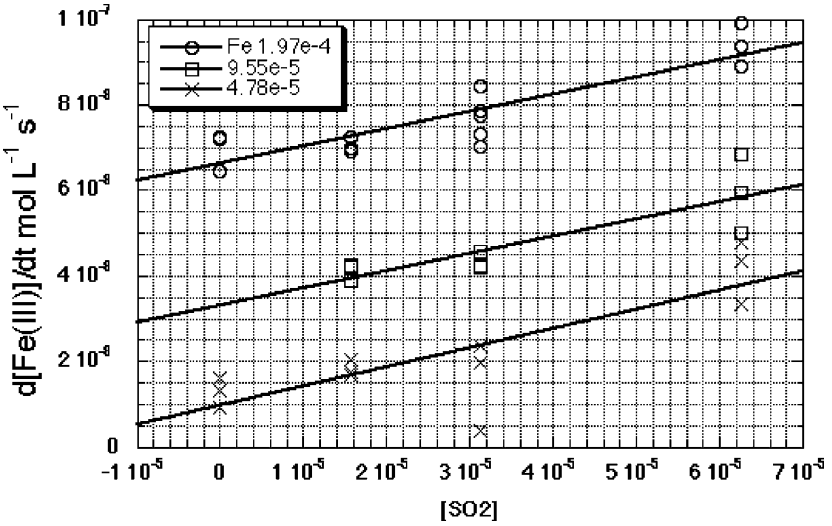

Fig. 6. Initial slope of [Fe(III)] vs. time plot, vs. [S(IV)] at constant initial [Fe(II)].

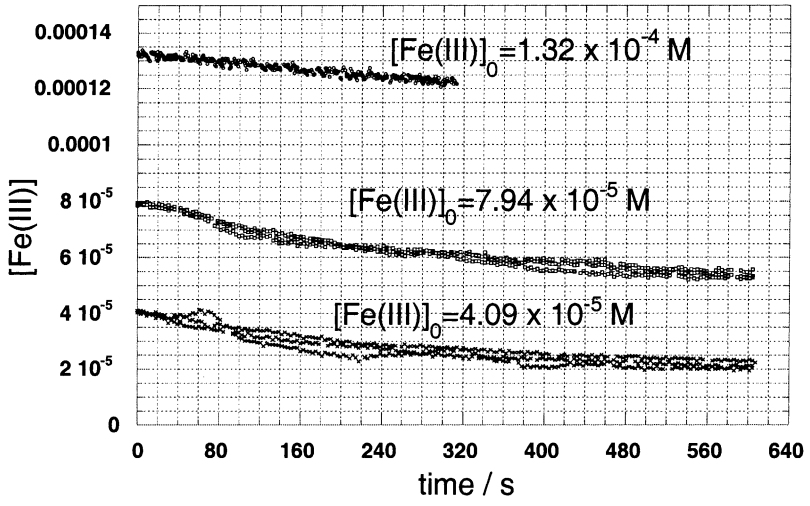

Fig. 7. Decrease of [Fe(III)] with time during photolysis of [Fe(III)] in 98% sulfuric acid.

4. Discussion

A likely primary process involving Fe(III) in our system is

$$FeHSO_4^{2+} + h\nu \rightarrow Fe^{2+} + H^+ + SO_4^- \quad (2)$$

Because the SO_4^- radical reacts very rapidly with Fe^{2+} to produce Fe^{3+} (see reaction 8 in Table 1) it is essential for the products of reaction 2 to have enough kinetic energy to escape from the initial solvent cage in order for this process to be important. The measured quantum yield of the analogous process involving $FeSO_4^+$, in dilute aqueous solution, varies from 1.5×10^{-3} to 7.5×10^{-3} between 350 and 280 nm, the yield increasing with decreasing wavelength [10]. The molar absorption coefficient at 248 nm is 6100 L (mol s)$^{-1}$ for Fe(III) in 98% acid. On the basis of an extrapolation of the 350 and 248 nm results, we estimate the quantum yield for process 2 at 248 nm to be about 0.01.

With SO_2 present we can also expect to have

$$HSO_3^- + h\nu \rightarrow H + SO_3^- \quad (3)$$

where the quantum yield for process 3 in aqueous solution has been measured as 0.19 at 213.9 nm [10]. The molar absorption coefficient in 98% acid at 248 nm is 40 L (mol cm)$^{-1}$.

A possible primary process involving Fe(II) is

$$Fe^{2+} + h\nu \rightarrow Fe^{3+} + e^-; \quad H^+ + e^- \rightarrow H \quad (4)$$

for which Papp and coworkers [14] have measured separate quantum yields at 253.7 nm for the Fe(II) species Fe^{2+} (aq), $FeSO_4$ (aq), and $FeHSO_4$ (aq) as 0.15–0.16, 0.30 and 0.67, respectively. In [8], this primary process was neglected because of the absence of measurable light absorption by Fe(II) in concentrated sulfuric acid. This omission is now considered to have been incorrect, because the higher concentration of Fe(II) and the relatively high quantum yield of process 4 compensate for the weakness of the absorption.

On the basis of the molar absorption coefficients and quantum yields given above, photolysis rate coefficients at 248 nm for processes 2–4 are in the approximate ratios 20:3:1. We used these ratios in our numerical calculations.

In strong acid, the solvated electron resulting from primary process 4 will rapidly be converted into a free hydrogen atom, as indicated. The hydrogen atoms from (3) and (4) can reduce Fe^{3+} to Fe^{2+}, or will form HO_2 if dissolved oxygen is available. Because HO_2 is a relatively long-lived species, it should then be possible to produce hydroxyl and HSO_4^- radicals by reaction with HSO_3^-, after which the OH could oxidize any available species, such as S(IV), Fe(II), or CO. Because it involves HSO_3^- rather than HSO_4^-, this process is not ruled out by the known high stability of sulfuric acid in the presence of ionizing radiation (cf. the Fricke dosimeter). The slightly equivocal effect of adding sulfite in the present experiments can be rationalized in terms of competition between the introduction of the new primary process 3 and removal of Fe(III) either by displacement of the equilibrium (1) or by reduction to Fe(II) with atomic hydrogen.

A basic mechanism for our system consists of the set of reactions given in Table 1, where species whose concentration is considered to be buffered are omitted, with the exception of HSO_4^-, and the nature of the complex ions containing Fe(II) and Fe(III) is not specified. Rate constants for the most important reactions in the set are taken from [10]. Other rate constants have been estimated with what we consider to be sufficient accuracy for numerical modeling of the system. Estimated values are shown simply as a power of 10, with no multiplier. Photolysis rates are set equal to the ratios calculated above. The reverse of reaction 20, which is the major thermal source for sulfite radicals in aqueous solution [10]and so could augment process 2, is not included here.

Model calculations have been done for this mechanism with the set of initial concentrations shown in Table 2, using a fourth-order Runge-Kutta integration routine with adaptive step-size, based mainly on the discussion in the book

Table 1
Processes included in the model calculations

2	$Fe(III) + h\nu \rightarrow Fe(II) + SO_4^-$	$J_2 = 20\,s^{-1}$
3	$HSO_3^- + h\nu \rightarrow H + SO_3^-$	$J_3 = 3\,s^{-1}$
4	$Fe(II) + h\nu \rightarrow Fe(III) + H$	$J_4 = 1\,s^{-1}$
5	$HSO_3^- + SO_4^- \rightarrow HSO_4^- + SO_3^-$	$k_5 = 7 \times 10^8$ L (mol s)$^{-1}$
6	$SO_3^- + O_2 \rightarrow SO_5^-$	$k_6 = 2.5 \times 10^9$ L (mol s)$^{-1}$
7	$H + O_2 \rightarrow HO_2$	$k_7 = 10^9$ L (mol s)$^{-1}$
8	$Fe(II) + SO_4^- \rightarrow Fe(III) + HSO_4^-$	$k_8 = 1 \times 10^8$ L (mol s)$^{-1}$
9	$Fe(II) + SO_5^- \rightarrow Fe(III) + HSO_5^-$	$k_9 = 1 \times 10^7$ L (mol s)$^{-1}$
10	$Fe(II) + HSO_5^- \rightarrow Fe(III) + SO_4^-$	$k_{10} = 3 \times 10^2$ L (mol s)$^{-1}$
11	$CO + HSO_5^- \rightarrow CO_2 + HSO_4^-$	$k_{11} = 10^3$ L (mol s)$^{-1}$
12	$HSO_3^- + SO_5^- \rightarrow SO_4^- + HSO_4^-$	$k_{12} = 3 \times 10^2$ L (mol s)$^{-1}$
13	$HSO_3^- + SO_5^- \rightarrow SO_3^- + HSO_5^-$	$k_{13} = 8.1 \times 10^3$ L (mol s)$^{-1}$
14	$Fe(III) + H \rightarrow Fe(II)$	$k_{14} = 10^9$ L (mol s)$^{-1}$
15	$Fe(II) + OH \rightarrow Fe(III)$	$k_{15} = 10^8$ L (mol s)$^{-1}$
16	$HSO_3^- + HSO_5^- \rightarrow 2HSO_4^-$	$k_{16} = 3 \times 10^2$ L (mol s)$^{-1}$
17	$H + SO_4^- \rightarrow HSO_4^-$	$k_{17} = 1 \times 10^{10}$ L (mol s)$^{-1}$
18	$H + SO_3^- \rightarrow HSO_3^-$	$k_{18} = 10^9$ L (mol s)$^{-1}$
19	$H + SO_5^- \rightarrow HSO_5^-$	$k_{19} = 10^9$ L (mol s)$^{-1}$
20	$Fe(II) + SO_3^- \rightarrow Fe(III) + HSO_3^-$	$k_{20} = 4 \times 10^7$ L (mol s)$^{-1}$
21	$OH + HSO_3^- \rightarrow SO_3^-$	$k_{21} = 3 \times 10^9$ L (mol s)$^{-1}$
22	$OH + HSO_4^- \rightarrow SO_4^-$	$k_{22} = 10^5$ L (mol s)$^{-1}$
23	$OH + HSO_5^- \rightarrow SO_5^-$	$k_{23} = 10^5$ L (mol s)$^{-1}$
24	$OH + CO \rightarrow H + CO_2$	$k_{24} = 10^5$ L (mol s)$^{-1}$
25	$HO_2 + HSO_3^- \rightarrow OH + HSO_4^-$	$k_{25} = 10^3$ L (mol s)$^{-1}$
26	$HO_2 + SO_3^- \rightarrow O_2 + HSO_3^-$	$k_{26} = 10^4$ L (mol s)$^{-1}$

Table 2
Initial concentrations (mol L^{-1}) used in the model calculations, except for Fig. 12, where the initial concentration of Fe(II) was set to zero

Fe(III)	1×10^{-5}
Fe(II)	4×10^{-5}
HSO_3^-	1×10^{-5}
HSO_4^-	0.1
O_2	1×10^{-5}
CO	1×10^{-5}

by Press et al. [15] with the tolerance (maximum disagreement between the results of a single time step and of two successive half-steps) set at one part in 10^7 [16]. The results of a calculation with all three primary processes included are shown in Fig. 8. Results with only primary process 2 are shown in Fig. 9. Results with only primary process 3 are shown in Fig. 10, and results with only primary process 4 in Fig. 11. Results using all three primary processes for a system which initially contains Fe(III) without Fe(II), are shown in Fig. 12. In these graphs, the concentration–time curve for each species has been scaled so that the maximum value is unity; the scaling factors are given in the figure captions. The time-scale of the experiments was much longer than the time-scale of the simulations because of the very low duty-cycle of the KrF laser (nominal pulse duration 50 ns).

The results in Figs. 8–11 show that the contribution of process 2 to the overall rate of conversion of Fe(II) to Fe(III) in our system is very small (note that the concentration of Fe(III) initially decreases in Fig. 9), that the contributions of processes 3 and 4 are of comparable magnitude, and that process 3 alone is sufficient to initiate the series of photochemical reactions that leads ultimately to removal of CO and O_2, in the absence of any iron salts. The initial decrease in the concentration of Fe(III) that is seen in Fig. 9 becomes the main feature of the observations when most or all of the iron is initially present as Fe(III). The results in Fig. 12, with the initial concentration of Fe(II) set to zero, show a decrease in Fe(III), similar to those in Fig. 7, followed by an increase when the concentration of Fe(II) has built up sufficiently for process 4 to predominate. As in the experiments, the change from removing to producing Fe(III) occurs when about one-third of the iron is present as Fe(III). It is noticeable that the removal of O_2 and formation of CO_2 begin at time zero, when all of the iron is present as Fe(III).

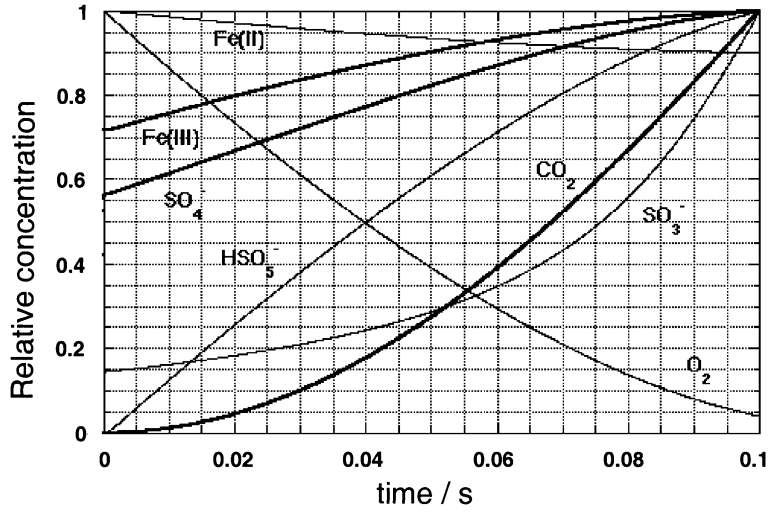

Fig. 8. Results of model calculation with all three primary processes. Scaling factors: 7.87E+04, 2.21E+07, 1.60E+07, 1.00E+05, 3.62E+05, 1.39E+05, 1.97E+08 for Fe(III), SO_4^-, SO_3^-, O_2, SO_5^-, HSO_5^-, and CO_2, respectively.

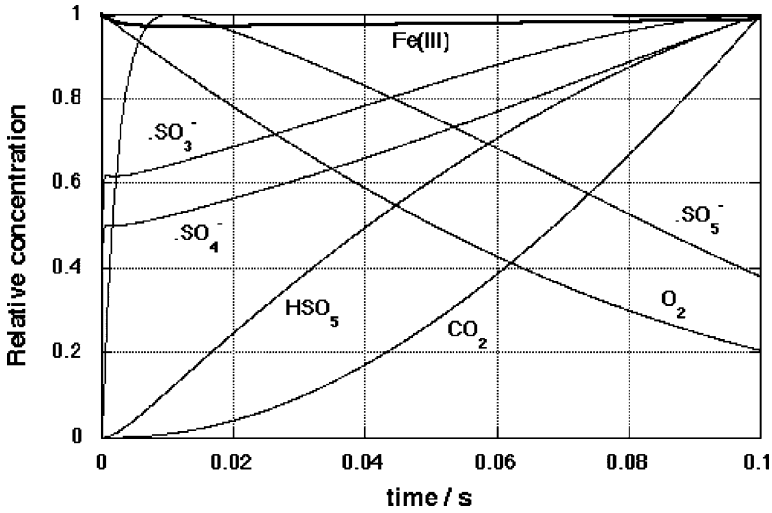

Fig. 9. Results of model calculation with Fe(III) primary process only. Scaling factors: 9.42E+04, 1.86E+07, 1.09E+08, 1.00E+05, 3.45E+07, 1.02E+05, 3.58E+06 for Fe(III), SO_4^-, SO_3^-, O_2, SO_5^-, HSO_5^-, and CO_2, respectively.

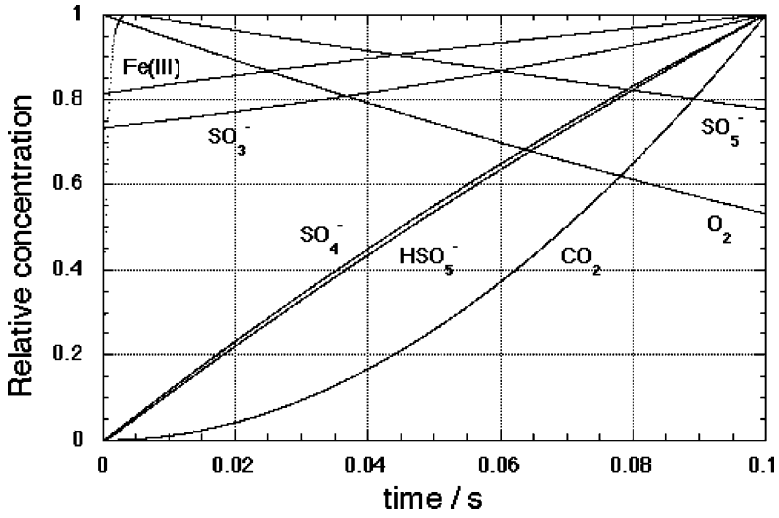

Fig. 10. Results of model calculation with S(IV) primary process only. Scaling factors: 6.90E+04, 9.39E+10, 1.62E+08, 1.00E+05, 1.45E+08, 2.00E+05, 1.10E+08 for Fe(III), SO_4^-, SO_3^-, O_2, SO_5^-, HSO_5^-, and CO_2, respectively.

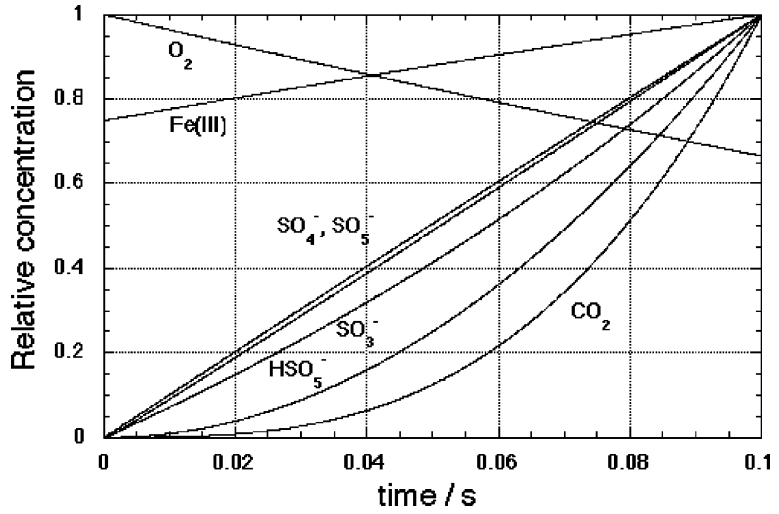

Fig. 11. Results of model calculation with S(IV) primary process only. Scaling factors: 5.52E+04, 1.30E+11, 9.41E+10, 1.00E+05, 7.95E+10, 1.35E+08, 1.08E+11 for Fe(III), SO_4^-, SO_3^-, O_2, SO_5^-, HSO_5^-, and CO_2, respectively.

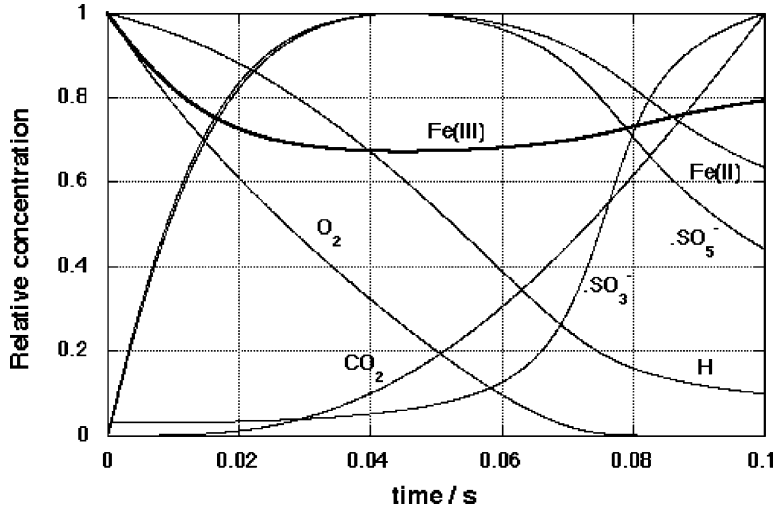

Fig. 12. Results of model calculations with the initial concentration of Fe(II) set to zero. Scaling factors: 1.00E+05, 3.05E+05, 1.72E+06, 3.305E+06, 6.75E+08, 1.00E+05, 2.81E+05, 2.50E+08 for Fe(III), Fe(II), SO_4^-, SO_3^-, H, O_2, SO_5^-, and CO_2, respectively.

In relation to the atmosphere of Venus, the processes considered here comprise a plausible mechanism for regeneration of CO_2 in the presence or absence of dissolved iron salts. We can identify the very fast reaction of the SO_3^- radical ion with O_2 as a prime candidate for the molecular oxygen sink at cloud-top level, and reaction of CO with HSO_5^- as a likely process for converting carbon monoxide to carbon dioxide. However, without detailed atmospheric modeling and inclusion of transport processes, it is not possible to decide whether these reactions are dominant on Venus, or merely provide an essential supplement to the mechanisms of Prinn [3]and Yung and DeMore [4]. More experimental data are needed on the concentrations of metal salts in the aerosol near the cloud-tops on Venus, on the speciation of S(IV), Fe(II) and Fe(III) in concentrated sulfuric acid, and on rate constants and quantum yields in concentrated and dilute sulfuric acid, both at room temperature and at 250 K. Also, there is clearly a need for modelers to begin to incorporate cloud photochemistry into their models of the upper-atmosphere of Venus.

Acknowledgements

This work was supported by the Marsden fund. We are grateful to C.T. Mills for helpful discussions.

References

[1] V.A. Krasnopolsky, Photochemistry of the Atmospheres of Mars and Venus, Springer, Berlin, 1986.
[2] P. Connes, J. Connes, L.D. Kaplan, W.S. Benedict, Astrophys. J. 147 (1968) 1230.
[3] R.G. Prinn, J. Atmos. Sci. 28 (1971) 1058.
[4] Y.L. Yung, W.B. DeMore, Icarus 511 (1982) 199.
[5] C.T. Mills, L.F. Phillips, J. Photochem. Photobiol. A: Chem. 74 (1993) 7.
[6] C.T. Mills, G.A. Rowland, J. Westergren, L.F. Phillips, J. Photochem. Photobiol. A: Chem. 93 (1996) 83.
[7] S.J. Wrenn, L.J. Butler, G.A. Rowland, C.J.H. Knox, L.F. Phillips, J. Photochem. Photobiol. A: Chem. 129 (1999) 101.
[8] G.A. Rowland, L.F. Phillips, Geophys. Res. Lett. 27 (2000) 3301.
[9] R.K. Chang, J.H. Eickmans, W.-F. Hsieh, C.F. Wood, J.-Z. Zhang, J.-B. Zheng, Appl. Optics 27 (1988) 2377.
[10] P. Warneck (Ed.), Transport and chemical transformation of pollutants in the troposphere, in: Heterogeneous and Liquid-Phase Processes, vol. 2, Springer, Berlin, 1996.
[11] M. Liler, Reaction Mechanisms in Sulphuric Acid, Academic Press, New York, 1971.
[12] L. Brewer, J.B. Tellinghuisen, J. Chem. Phys. 54 (1971) 5133.
[13] M.H. Mariano, Anal. Chem. 40 (1968) 1662.
[14] L. Vincze, B. Kraut, S. Papp, Inorg. Chim. Acta 85 (1984) 89.
[15] W.H. Press, S.A. Teukolsky, W.H. Vetterling, B.P. Flannery, Numerical Recipes, 2nd ed., Cambridge University Press, Cambridge, 1992.
[16] The Macintosh application can be obtained from the URL http://www.chem.canterbury.ac.nz/people/academics/lfp.htm